Journal of Sol-Gel Science and Technology 36, 33–43, 2005

Low Cost Selective Solar Absorber Coatings: Characteristics of Carbon-In-Silica Synthesized with Sol-Gel Technique

G. KATUMBA*
Physics Department, University of Zimbabwe, P.O. Box MP 167, Mt. Pleasant, Harare, Zimbabwe
katumba@science.uz.ac.zw

J. LU
Microstructure Laboratory, Ångströmlaboratoriet, Box 534, 751 21 Uppsala, Sweden

L. OLUMEKOR
Physics Department, University of Zimbabwe, P.O. Box MP 167, Mt. Pleasant, Harare, Zimbabwe

G. WESTIN
Department of Material Chemistry, Ångströmlaboratoriet, Box 538, 751 21 Uppsala, Sweden

E. WÄCKELGÅRD
Solid State Physics, Ångströmlaboratoriet, Box 534, 751 21 Uppsala, Sweden

Received November 18, 2004; Accepted June 21, 2005

Abstract. Carbon-silica composite films have been fabricated using sol-gel synthesis of silica-carbon precursor composites, followed by carbonization in an inert atmosphere. Four categories of samples were studied. These were the tetraethyl orthosilicate-only (TEOS-only), methyl trimethoxysilane (MTES), acetic acid anhydride (Ac_2O) and soot (SOOT) samples. The carbon-silica films, spin-coated on aluminium and steel substrates, have been investigated for selective solar absorber functionality. Optical measurements were performed on these samples to determine solar absorptance and thermal emittance of each. The morphology of the films was studied by electron microscopy. Electron energy-loss spectroscopy (EELS) mapping was used to determine the carbon distribution. An optimum performance of 0.88 for solar absorptance and 0.41 for thermal emittance has been achieved. The sol-gel technique produced films with very flat surfaces and uniform thicknesses in the 1 μm range. The fine structure showed homogeneous mixing of the carbon and silica in the TEOS-only samples while the separate additions of MTES and Ac_2O resulted in segregation of composition of the silica and carbon at nano-scale. The addition of 20 wt% MTES or 15 wt% Ac_2O to the TEOS-only sols also helped to reduce the cracks in the TEOS-only samples. The addition of soot in place of the carbon precursor did not yield a net advantage.

Keywords: carbon-silica synthesis, selective solar absorbers

*To whom all correspondence should be addressed.

1. Introduction

The investigation and development of carbon-silica composites has been going on for some time [1–7]. Different applications have emanated from these studies. Examples are the use of carbon-silica composites as adsorbents [1–3], biosensors [4], templates [5, 6] and solar absorbers [7], just to mention a few. The latter application is very pertinent to developing countries that are in need of cleaner and low cost energy. It is the thrust of this work to contribute more information on practical selective solar absorber materials that are economical and environmental friendly without compromising their operational efficiency.

Several different design principles and physical mechanisms can be exploited in the production of a selectively solar-absorbing surface. The desired spectral selectivity is a high absorptance in the solar spectral range between 0.3 and 3 μm and a low thermal emittance in the infrared (IR) wavelength range between 3 and 50 μm. The simplest method would be to use a material whose intrinsic radiative properties have the desired spectral selectivity. Such intrinsic materials are known to exist but they have not been useful [8]. A spectrally selective solar absorber can also be produced by combining two layers that have different optical properties. This is usually referred to as a tandem absorber. A dielectric coating with high solar absorptance and high infrared transmittance on top of a non-selective highly reflecting metal constitute one type of a tandem absorber. A description of other types of tandem absorbers is given by Wäckelgård et al. [8].

The concept of using solar absorbing nanoparticles embedded in a dielectric matrix in tandem with a metal substrate has been investigated both theoretically and practically by a number of authors [9–13]. Most of the authors investigated coating systems that contained metallic absorber particles embedded in a dielectric matrix. Matsai et al. [7] investigated carbon-in-silica in bulk form. To the best of our knowledge no comprehensive study has been conducted on thin coatings of carbon-in-silica on metal substrates, especially for selective solar absorber applications.

Three major properties led to the study of the carbon-in-silica tandem selective solar absorber. First, both carbon and silica are abundant, environmental friendly and stable materials. In contrast, metallic absorber particles used hitherto are likely to degrade over a long period of use when oxidation occurs, especially in high temperature and high humidity environments. A second attraction is that theoretical calculations [14] have shown that carbon particles of sufficiently small size of approximately 10 nm or less have a high absorption cross-section for UV-VIS radiation. The other major attraction is that the carbon-silica composite can be synthesized easily via a sol-gel technique. This technique is cost effective because the cost of capital equipment is much less compared to other techniques such as sputtering used mainly for industrial production. Moreover, the sol-gel technique affords easier control of coating parameters such as absorber particle size, particle size distribution, homogeneity and thickness. It also offers the opportunity to adapt and utilize industrial applications such as spray-painting that are already in use for larger surface area coatings.

Most sols are made by hydrolysis and polymerization of alkoxides such as TEOS. A concise review of sol-gel processing is given by Rabinovich [15]. Livage et al. [16] discussed sol-gel chemistry for optical materials. These authors raised issues that are pertinent to the current study. These issues concern the mechanical fracturing that characterise most acid-catalyzed silica gels upon drying. While Rabinovich [15] suggested a complex and expensive approach to minimize the cracking by drying in a variety of gas media, a more economic procedure is being suggested here.

In our approach TEOS and sucrose (SUC) are the silica and carbon precursors, respectively. The process involves synthesizing the silica-carbon precursor sol, spin-coating the sol on a metal substrate and carbonization in an inert environment. The achievement of crack-free coatings was attempted via a chemical process of organic modification of the inorganic silica, to give rise to the so-called ORMOSIL [16]. An alternative route to achieve a similar result made use of attachment of side-groups to the carbon precursor prior to the hydrolysis, condensation and carbonization processes. The intention was that the side-groups would minimize cracks in the coatings by occupying most of the pore volume in the silica thereby minimizing shrinkage.

2. Experimental

2.1. Substrate Preparation

Three types of substrates, namely specular aluminium, rough aluminium and stainless steel, were used. Each of the substrate measured approximately 55 mm square. Specular aluminium substrates were treated in

a chromic acid bath held at 80°C for 8 to 10 min to etch away a pre-deposited Al_2O_3 layer. The Al_2O_3 layer had to be removed in order to allow for the formation of carbon-in silica on aluminium, a two-layered tandem device that was desired. Rough aluminium substrates were treated in a phosphoric acid bath held at 60°C for about 20 min to also remove oxide layer that normally forms on aluminium in air. Stainless steel substrates were cleaned by dipping in a dilute nitric acid bath held at room temperature for about 20 min to remove a protective oxide layer on the steel. All reagents used in substrate cleaning were obtained from Merck, Germany and all were p.a. grade. After these different acid treatments all the substrates were rinsed thoroughly in distilled water and then dried by blowing with nitrogen gas.

2.2. *Sample Preparation*

Samples for this study were made from silica sols based on acid-catalysis of TEOS and water that were impregnated with SUC. Hydrochloric acid (HCl) was used to acidify the water. All chemicals used in this preparation were from Aldrich and were of the p.a. grade.

The sample preparation was essentially a three-step process as shown in Fig. 1.

The hydrolysis and polymerization processes were initiated at pH 2. Sucrose was first dissolved in acidic water in a plastic container, and then TEOS was added. Contents were stirred continuously at room temperature until a homogenized sol formed. Three other routes to Step II were taken by the addition of various amounts of MTES, Ac_2O, or SOOT, in turn. These routes were taken to minimise the cracks that developed after the carbonization process of samples made from TEOS only, and/or to improve the selectivity. The relative quantities of TEOS, H_2O (acidic), SUC, MTES and Ac_2O used in the different sols are given in Table 1.

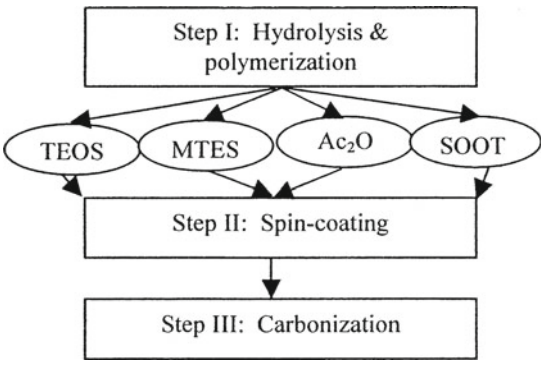

Figure 1. Sample preparation processes showing the four routes used between steps I and II.

Table 1. Chemical compositions used in the preparation of sols.

wt.% MTES or Ac_2O (relative to TEOS)	Weight (g)			
	TEOS	MTES or Ac_2O	H_2O	SUC
0	12	0	9	6
			9	9
			9	11
			9	12
10	10.8	1.2	9	4
			9	6
			9	9
			9	11
15	10.2	1.8	9	4
			9	6
			9	9
			9	11
20	9.6	2.4	9	4
			9	6
			9	9
			9	11
30	8.4	3.6	9	4
			9	6
			9	9
			9	11

The SOOT route was made by addition of 0.05 g of soot to the TEOS-only sol with H_2O:SUC weight ratio equal to 9:11. The mixture was vigorously stirred to make a homogeneous suspension.

Step II involved spin coating of the sols onto the different substrates. The spin coating was performed initially at rates of 2000, 3000, 3600, 4000 and 5000 revolutions per minute (rpm). An optimum speed of 4000 ± 100 rpm was used for the rest of the experiment. An explanation of how the optimum spin coating speed was arrived at is given in Section 3.2.

In Step III, the spin-coated substrates were immediately placed in a quartz glass tube and then flushed with nitrogen gas for 30 min. to reduce the amount of oxygen in the tube before the carbonization process was

started. The carbonization process, carried out in inert atmosphere of nitrogen gas, involved placing the glass tube with the contents in a split-tube furnace. The furnace temperature was raised to 550°C at 5°C min^{-1}, maintained at 550°C for 60 min. and then cooled to 30°C at 20°C min^{-1}. Samples were ready for characterization thereafter.

2.3. Optical Characterization

The near normal spectral hemispherical reflectance, R, of the prepared samples was measured in the wavelength interval 0.3 to 20.0 μm. A Perkin Elmer Lambda 900 double beam spectrophotometer was used for measurements in the 0.3 to 2.5 μm interval. A Labsphere spectralon reference was used for baseline measurements on this instrument. A single beam FTIR Bomem-Michelson 110 spectrophotometer was used for measurements in the 2.5 to 20 μm interval. A specular vacuum-evaporated aluminium film on silicon was used for reference measurements. The measurements were combined to form one spectrum in a MATLAB program.

Solar absorptance, α_{sol}, and thermal emittance, $\varepsilon_{\text{therm}}$, both defined as follows for normal angle of incidence, were calculated according to Eqs. (1) and (2), respectively. The solar absorptance is defined as a weighted fraction of the absorbed radiation to that incident on a surface. The direct normal spectral solar irradiance, $I_{\text{sol}}(\lambda)$, is defined by the ISO standard 9845-1 (1992) for air mass 1.5. Equation (1) is thus:

$$\alpha_{\text{sol}} = \frac{\int_{0.3}^{2.5} I_{\text{sol}}(\lambda)(1 - R(\lambda))\, d\lambda}{\int_{0.3}^{2.5} I_{\text{sol}}(\lambda)\, d\lambda} \tag{1}$$

The thermal emittance is similarly defined against the spectral Planck blackbody radiation, $I_P(\lambda)$ at 373 K as:

$$\varepsilon_{\text{therm}} = \frac{\int_{2.5}^{20} I_P(\lambda)(1 - R(\lambda))\, d\lambda}{\int_{2.5}^{20} I_P(\lambda)\, d\lambda}. \tag{2}$$

2.4. Structural Characterization

2.4.1. SEM and X-HRTEM. The surface morphology of the samples in the TEOS-only, MTES and Ac_2O categories were investigated with a Zeiss DSM 960A Scanning Electron Microscope (SEM).

The structure of the above samples was studied by cross-sectional high-resolution transmission electron microscopy (X-HRTEM). A field-emission-gun Technai F30 ST operated at 300 kV with a point resolution of 0.205 nm and equipped with a Gatan Imaging Filter was used for this study.

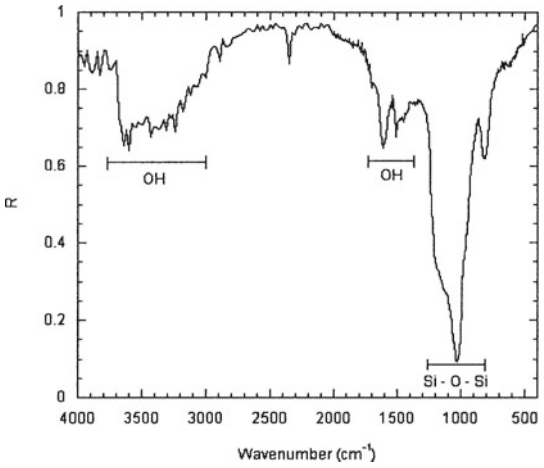

Figure 2. Identification of chemical bonds in the absorber composite layer from an FTIR reflectance spectrum.

3. Results and Discussion

The hemispherical reflectance spectra of the samples used for the different investigations in this work are shown in Figs. 2 to 9. All the spectra belong to samples prepared on rough aluminium substrates. Several samples were made at the same conditions to ensure reproducibility in the results. The different aspects investigated ensue in Sections 3.1 to 3.6.

3.1. Identification of Chemical Bonds

Characteristic chemical bonds in the coatings were identified from the FTIR reflectance spectrum. This spectrum, given in Fig. 2, typifies the rest of the samples made in this work.

Three distinct absorption bands are observed. The major band at approximately 1050 cm^{-1} is assigned to stretching vibrations of Si—O—Si or Si—O—X, where X represents ethoxy groups bonded to silicon [17, 18]. The shoulder at about 1200 cm^{-1} is assigned to either the transverse optical mode of the out of phase mode of

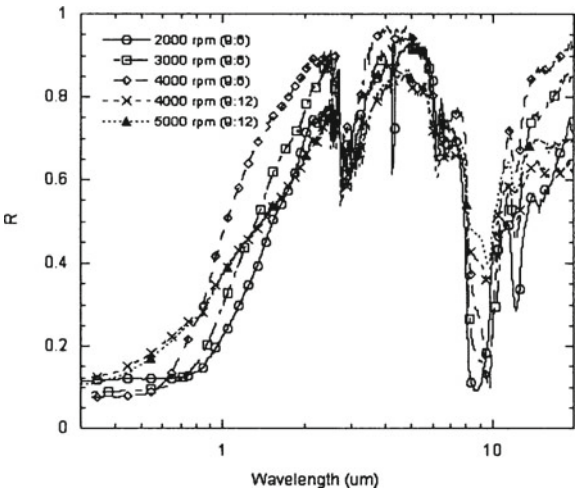

Figure 3. Effect of speed of spin coating showing the movement of the transition step from low to high reflectance in the VIS/NIR wavelength range.

the asymmetric vibration, or to the longitudinal optical mode of the high frequency vibration of SiO_2 [17]. On the other side of the major absorption band, at about 900 cm^{-1}, is an absorption band that can be assigned to the stretching vibration of Si—OH or Si—O^- groups. A rather broad absorption band, situated between 3000 and 3600 cm^{-1}, and another one around 1600 cm^{-1} are assigned to O—H stretching and O—H bending vibrations, respectively [17, 18]. The latter absorption bands indicate the hydrophilic nature of the sol-gel synthesized silica.

3.2. *Effect of Speed of Spin Coating*

The spin rate of the spin-coating process was optimised using rough aluminium substrates. This was investigated for a sol that had a TEOS:H_2O:SUC weight ratio of 12:9:6 at rotation speeds of 2000, 3000 and 4000 rpm. Speeds of 4000 and 5000 rpm for a 12:9:12 TEOS:H_2O:SUC ratio were used for comparison.

It can be observed that for the 12:9:6 ratio samples, the transition from low to high reflectance moved progressively towards shorter wavelengths as the speed was increased from 2000 to 4000 rpm. This suggests that higher spin coating speeds results in thinner films. There is therefore a qualitative agreement with observations of Thomas [19]. However, the same cannot be said for the samples from a more viscous sol with 12 g SUC. Here there is no detectable difference for speeds of 4000 and 5000 rpm. This is probably because the viscosity of the sol becomes too high to make any noticeable difference.

An interesting observation for the 6 g SUC samples is that for wavelengths less than 0.6 μm the reflectance decreases with increasing speed of spin-coating. This behaviour is not well understood but it may be explained by a particle-size effect computed by Etherden et al. [14] in the scattering and absorption cross-sections of carbon particles. It must be pointed out that Etherden et. al. assumed a spherical shape for the carbon particles in the computations. This is not necessarily the case for our samples, which showed chain-like structures for both the carbon and silica components (see results in Section 4).

For wavelengths longer than 10 μm, the reflectance increases with increasing spin-coating speed. The net result is that samples with relative lower emittance can be obtained at higher speeds of rotation. Following this argument an optimum spin coating speed was determined by calculating the ratio of solar absorptance to thermal emittance ($\alpha_{sol}/\varepsilon_{therm}$) for samples deposited at the five coating speeds stated earlier. The concentration and the maturity times of the TEOS-only sols used in this optimisation experiments were kept constant. The results of the $\alpha_{sol}/\varepsilon_{therm}$ calculations are presented in Table 2. The speed that had highest $\alpha_{sol}/\varepsilon_{therm}$ value was considered to be the optimum speed and a value of 4000 rpm was thus identified and used for the rest of the experiments.

3.3. *Effect of Amount of Carbon Precursor*

Figure 4 shows the variation of total reflectance with the amount of SUC in the sols. The investigation was done

Table 2. The dependence of the ratio of solar absorptance to thermal emittance with spin-coating speed.

Spin coating speed (rpm)	Sol maturity time (hrs)	Solar absorptance α_{sol}	Thermal emittance ε_{therm}	$\alpha_{sol}/\varepsilon_{therm}$
2 000	24	0.7771	0.4112	1.8898
3 000	24	0.7491	0.3511	2.1336
4 000	24	0.6707	0.2798	2.3971
2 000	48	0.7538	0.4164	1.8103
3 000	48	0.7351	0.3422	2.1420
4 000	48	0.6484	0.2847	2.2775
5 000	48	0.6969	0.3208	2.1724

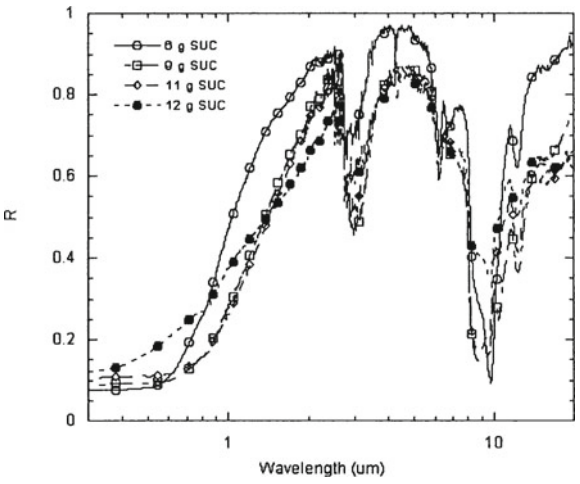

Figure 4. Effect of the amount of SUC in samples spin-coated at 4000 rpm.

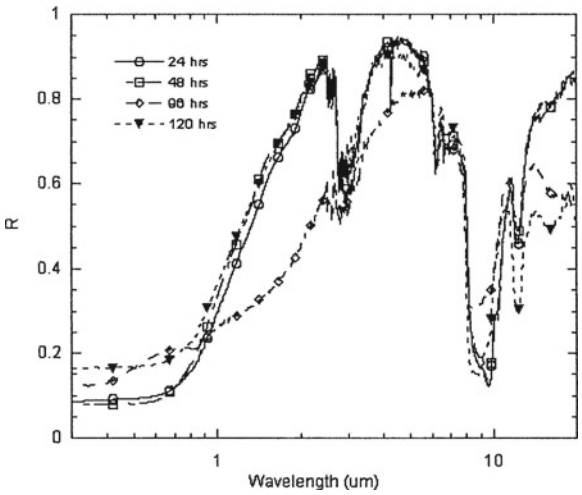

Figure 5. Effect of ageing time of sol for samples with 6 g SUC showing the changes in reflectance in the UV-VIS wavelength range.

with 6, 9, 11 and 12 g of SUC for a fixed TEOS:H_2O ratio of 12:9. The low to high reflectance transition appears to move towards an apparent limit of 2 μm with increasing amount of SUC.

It is striking that for wavelengths less than 0.8 μm, the reflectance increased with increasing amount of SUC. It was expected that an increase in SUC would lead to more absorption, and hence lower reflectance, in the UV-VIS interval. This behaviour suggests that when the amount of SUC is low the resultant carbon chains in the silica matrix have on average a small size and more uniform distribution as shown in Fig. 13(a) and therefore would have a higher absorption cross-section. When the amount of SUC was increased the resultant carbon chains probably agglomerated to form larger aggregates with a large scattering cross-section that resulted in higher reflectance. The gain in absorptance in the UV-VIS for the low SUC samples was accompanied by a loss in absorptance in the 0.8 to 2.0 μm interval.

In the NIR and IR regions the reflectance of the samples with low SUC content is higher than that of samples with higher SUC content. The reason for this could probably be that samples of low SUC content were thinner than those of higher SUC content. This is thought to be purely a viscosity effect of the sol during the spin-coating process. The net result of this behaviour is a lower thermal emittance by samples with low SUC content.

The foregoing arguments point to the fact that an optimum of SUC content had to be sought. An optimum for samples with high-absorptance and low-emittance was chosen to be 11 g SUC.

3.4. *Effect of Sol Ageing Time*

The ageing characteristics of the TEOS:H_2O:SUC sols were investigated. Total reflectance spectra of samples spin-coated at different times from a sol with 6 g SUC were considered. The spectra for 24, 48, 96 and 120 h are presented in Fig. 5. The 24- and 48 h spectra have the transition from low to high reflectance at about 1.5 μm and the reflectance for wavelengths less than 0.8 μm is just under 8%. The spectrum for 96 h is interesting in two aspects. One aspect is that the transition from low to high reflectance is at about 2 μm and the other is that the film showed some interference fringes in the UV-VIS interval; a substrate contribution is the likely cause. Though uncertain, it seems that the film is thinner than those for 24 and 48-h samples. However, the overall reflectance for the 96-h sample is rather low, and this leads to a higher emittance drawback. Further investigation with 96-h samples may be necessary to establish the exact cause of this behaviour. After 120 h the sol is no longer suitable for spin coating because both the absorption and the emittance deteriorate significantly.

From the above observations it is clear that for optimum results of α/ε it is best to spin-coat the pure silica sol at times between 24 and 48 h of ageing.

3.5. *Minimization of Cracks in Samples*

Samples made from acid-catalysed TEOS:H_2O:SUC sols showed severe cracking after heat treatment at 550°C for 1 h. Low ramp rates for the heating and cooling periods of 5 and 20°C per min, respectively, were used to avoid or minimise thermal shock during the heat treatment in a nitrogen gas environment. In spite of this precaution the samples still cracked. The sources of the cracks are not known very well. It is most probable that the cracks originate either from shrinkage in the film layer during the carbonisation process, or from a mismatch in the coefficients of thermal expansion of the film layer and the aluminium substrate, or from both sources. It is known that 99.99% pure aluminium has a coefficient of thermal expansion of 27.4 ppm K^{-1} at 500°C while that of a dry coating of carbon containing silica at the same temperature could not be found. Brinker and Scherer [20] suggested that at a critical thickness of 1 μm it is impossible to dry a sol-gel coating without cracks. However, there has been evidence of exceptional cases by Schlichting and Schmidt et al. [20], who dried films of thicknesses of 10 and 20 μm, respectively. The films used in this study are 1 to 1.4 μm thick, which is in the critical thickness range for drying without cracks. In the absence of measured coefficient of thermal expansion of the critical coating layer, and also with the coating being polymeric in nature, it is assumed that at a temperature of 550°C the coating layer is compliant enough to cater for any small mismatch in the coefficients of thermal expansion of the coating and the aluminium substrate.

The alternative was then to solve the problem of cracking from a shrinkage point of view. Two routes were taken to solve this problem. One route was the modification of the TEOS-only inorganic silica synthesis. The other route was the addition of small amounts of acetic anhydride to the TEOS-only sol.

3.5.1. Use of Organic-Inorganic Hybrid Silica. The use of organic material to minimise cracks in porous acid-catalysed silica is well known [15, 16]. When the organic groups are integrated into the silica matrix, they fill in the pores between the inorganic oxide chains. This results in low shrinkage of the matrix during heat-treatment. In this experiment MTES was chosen for this purpose and also for the fact that it has an affinity for water. The MTES would remove the water from the silica matrix. The water would eventually evaporate during the heat treatment. This results in an improvement of the emittance of the films because the OH absorption around 3 μm [18] would be reduced.

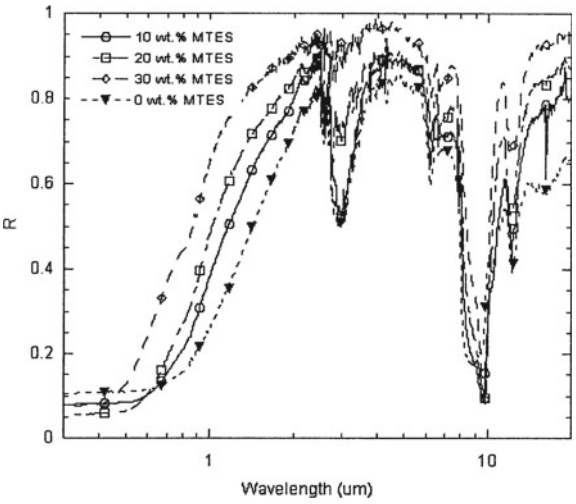

Figure 6. Effect of MTES on samples with H_2O:SUC ratio 9:11. It is clear the transition step moved towards shorter wavelengths with increase in MTES content.

Total reflectance spectra of samples of 10, 20 and 30 wt% MTES are shown in Fig. 6. The spectrum of a TEOS-only sample is included for comparison. Figure 6 shows that the transition from low to high reflectance moved towards the VIS wavelength interval with increase in the amount of MTES. Visually, the samples have a brown tinge, a departure from the blackness observed in the TEOS-only samples. As expected, the cracks and OH absorption gradually disappeared with increase in the amount of MTES. It was found that in the IR wavelength range the samples with the most MTES had the highest reflectance and hence the least emittance. In the UV-VIS wavelength range, samples with 20 wt% MTES had the least reflectance and hence the best absorptance of all MTES samples, although MTES samples had generally lower reflectance compared with the TEOS-only samples.

It could be concluded that an optimum amount of MTES that minimised the cracks without much deterioration of the absorptance and emittance characteristics of the samples is at 20 wt%.

3.5.2. Use of Acetic Acid Anhydride. Ac_2O is a highly mobile liquid that was used with a view to reduce the OH absorption present in the inorganic silica samples. It also minimised the cracking problem by

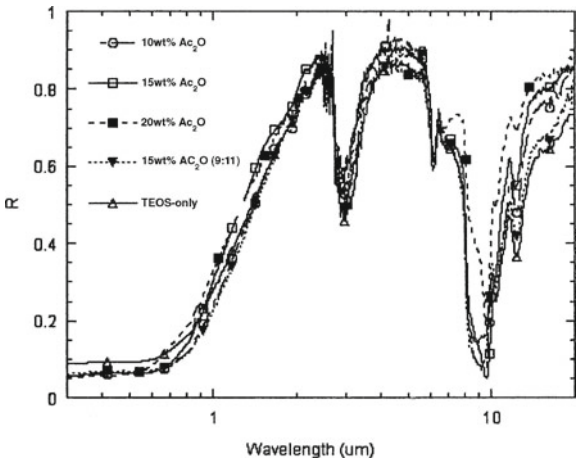

Figure 7. Effect of Ac_2O content samples with H_2O:SUC ratios of 9:9 and 9:11.

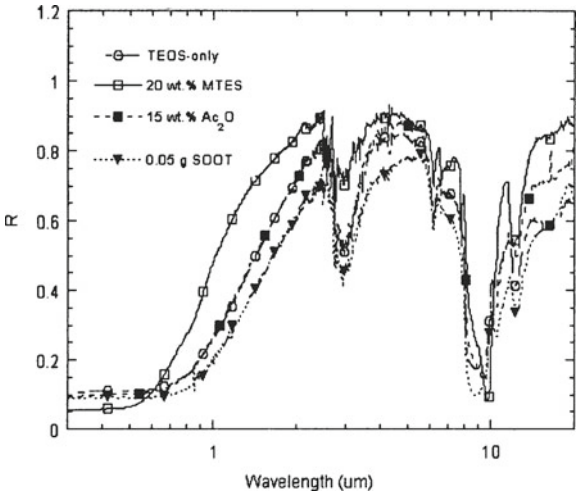

Figure 8. Effect of SOOT on the absorption and emittance characteristics compared to those of MTES and Ac_2O.

attachment of acetyl side-groups to the SUC molecules prior to carbonization. Ac_2O of 10, 15 and 20 wt% were added to the pure silica reagents with H_2O:SUC content of 9:9 and 9:11. The spectra of samples spin-coated from the Ac_2O samples are shown in Fig. 7. A graph from a TEOS-only sample is included for comparison. A comparison of spectra of samples with 9:9 H_2O:SUC concentration shows that the transition from low to high reflectance moves towards shorter wavelenghts with increase in Ac_2O content form 10 to 15 wt%. Addition of more SUC to 15 wt% Ac_2O moves the transition to longer wavelength. It is also worth to note that all Ac_2O samples had better absorptance in the UV-VIS interval than the TEOS only sample, irrespective of the SUC content. Visually, Ac_2O samples look qualitatively less black than TEOS-only samples.

The cracking in the film diminishes with increasing Ac_2O content but the absorptance in the UV-VIS gets slightly poorer due to the movement of the transition of low to high reflectance towards short wavelengths. An optimum of 15 wt% Ac_2O for a 9:9 H_20:SUC sol was determined. It was noted that the Ac_2O did not diminish the cracking as much as the MTES did.

3.6. *Effect of Soot*

The effect of the addition of soot particles is presented in Fig. 8. The addition of soot to a 9:11 TEOS-only sol before spin coating resulted in samples whose transition step was closer to 2 μm, the ideal point of crossover, than those without soot. This gain in absorptance was, however, accompanied by an undesirable increase in thermal emittance in the IR wavelength interval.

Figure 8 shows a comparison of the additives 20 wt% MTES and 15 wt% Ac_2O to TEOS-only samples. The Ac_2O samples appear to have an overall advantage over the MTES samples because the IR emittance is lower (higher IR reflectance) and the UV-VIS absorptance for the Ac_2O route is higher (lower UV-VIS reflectance). The apparent advantage of MTES is in the ability to minimise OH absorption better than Ac_2O around 3 μm.

3.7. *Limits of Absorptance and Emittance*

The various combinations of absorptance and emittance of the sample used in this investigation are shown in Fig. 9. This graph shows that the limit for absorptance is about 0.95 and that for emittance is about 0.1. The optimum figures achieved in a single sample are 0.88 for absorptance and 0.41 for thermal emittance calculated at 373 K. Comparative figures for similar carbon-in-silica absorbers are 0.93 for absorptance (probably for bulk surface) and 0.13 for thermal emittance (probably for a thin coating) at room temperature [7]. No comparative figures could be obtained for thin films of carbon-in-silica composite absorbers.

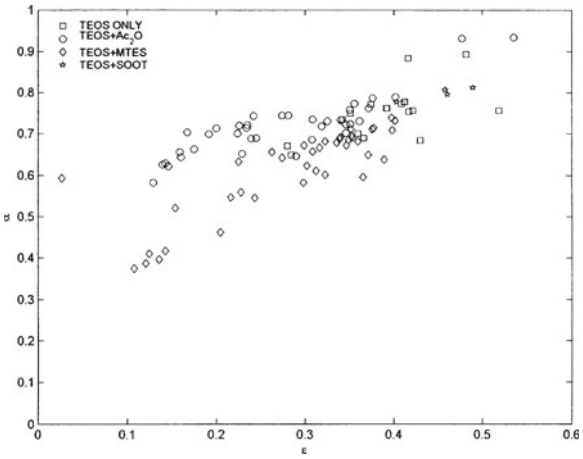

Figure 9. Scatter graph of absorptance and emittance of all types of samples used in the investigation.

4. SEM and X-HRTEM Results

4.1. SEM Results

The scanning electron microscopy (SEM) images are shown in Fig. 10. These figures were made with a secondary electron detector at a magnification of 200. A magnification of 200 allowed for the relative comparison of the severity of cracks in the TEOS-only, MTES and Ac_2O samples.

Figure 10(a) shows that the TEOS-only sample has numerous wide cracks of widths ranging from 9 to 12 μm. Figures 10(b) and (c) show that the MTES and Ac_2O samples both have fewer cracks and narrower fissures of about 2 to 6 μm. All the three images also show that the crack-free areas of the samples are fairly flat although there are noticeable differences between the three types of samples. The TEOS-only sample appears to show a homogeneous surface while the MTES and Ac_2O samples appear to have little segregation between the carbon and silica. This may be an indication of the modification of the silica chain network by the MTES and Ac_2O additives.

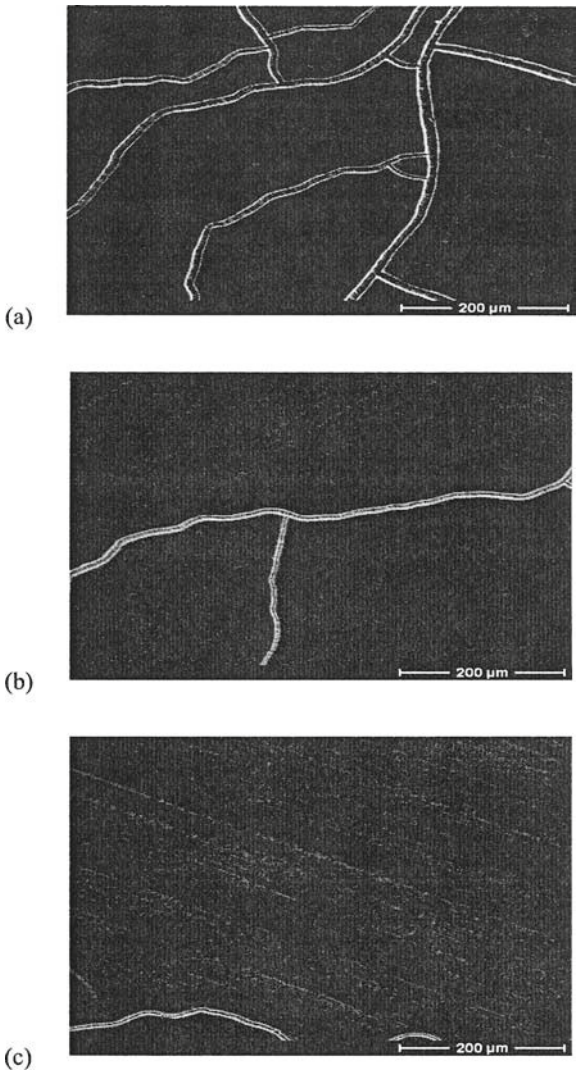

Figure 10. A typical distribution and size of cracks in (a) a TEOS-only sample, (b) an MTES sample and (c) an Ac_2O sample. All pictures were taken at 200X.

4.2. X-HRTEM Results

The images from cross-sectional high-resolution transmission electron microscopy (X-HRTEM) are shown in Figs. 11 to 14. Figure 11(a) shows that the TEOS-only film has a poor adherence while the other two films from MTES and Ac_2O in Fig. 12 possess an excellent adherence with the substrate. The transmission electron microscopy (TEM) observation also demonstrates that the TEOS-only film has a high porosity shown in Fig. 11(b). In contrast to the porous film, the films with MTES and Ac_2O contain a few cracks as shown in Fig. 12. Figure 12 also shows that MTES and Ac_2O films have a smooth surface and uniform thickness. The average thicknesses of the films are between 1 to 1.4 μm. Note that all the scale bars in Figs. 11 and 12 are 3 μm.

It seems that the MTES film (see Fig. 12(2)) has a slightly rougher interface than the interface of the

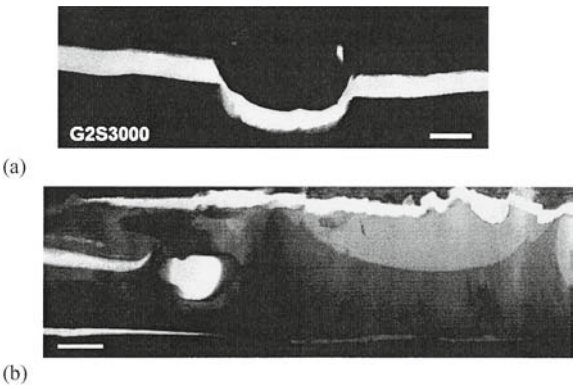

Figure 11. (a) A TEOS-only film peels off and creates a gap between the film and the substrate. The bright parts indicated the air gap between the substrate at the bottom and the film at the top. (b) The TEOS-only film showing a rough film surface and high porosity.

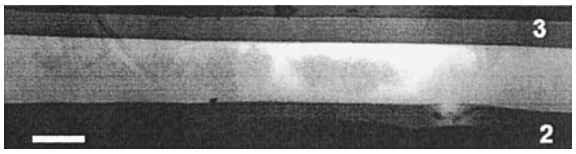

Figure 12. The bright field image of an MTES film (2) and an Ac_2O film (3). The images show that films have flat surface and uniform thickness.

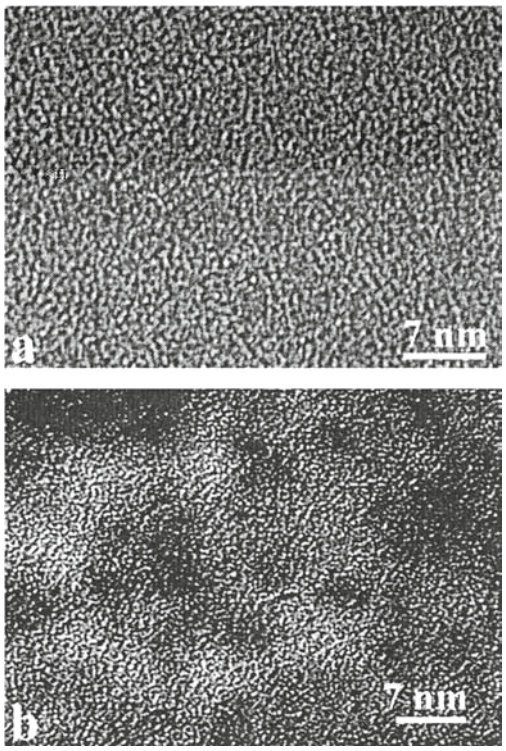

Figure 13. X-HRTEM images of (a) TEOS-only and (b) Ac_2O samples.

film from Ac_2O (see Fig. 12(3)). This could be a result from the different substrate surface structures prior to the deposition. X-HRTEM was also used to determine the fine structure of the films. Figure 13(a) clearly demonstrates that the TEOS-only film has a uniform composition distribution while Fig. 13(b) for the Ac_2O film exhibits a segregation of composition in nano-scale.

EELS mapping was used to determine the carbon distribution. The result is shown in Fig. 14. A carbon *K* peak was chosen to form the mapping. An energy window with 20 eV width was selected for the carbon mapping. The bright region in Fig. 14(b) corresponds to carbon or carbon-rich region.

5. Comments and Conclusions

This work has demonstrated that it is possible to produce low cost selective absorbers in thin film form using low cost and abundant materials like TEOS and sucrose. The optimum performance achieved in a single sample is 0.88 for absorptance and 0.41 for thermal emittance. An improvement of this performance is subject of further research.

A successful reduction of cracks in the carbon-silica composites has been achieved by the use of MTES and Ac_2O as organic modifiers of inorganic silica. An addition of 20 wt% MTES or 15 wt% Ac_2O resulted in films of optimum optical performance with minimal cracks. The samples with 20 wt% MTES had a solar absorptance of 0.74 and a thermal emittance of 0.30, while the corresponding values for samples with 15 wt% Ac_2O were 0.81 and 0.44, respectively.

Completely new and interesting structures of the sol-gel derived samples have been revealed in this study. A short chain-like structure of both the silica, forming the matrix, and the carbon, forming the absorber particles, is quite evident. Homogeneity of the sol-gel synthesized carbon-silica composite films at nano-scale is very encouraging. The excellent film-substrate adhesion and uniform film thickness could make sol-gel synthesis a low cost production technique for selective solar absorbers.

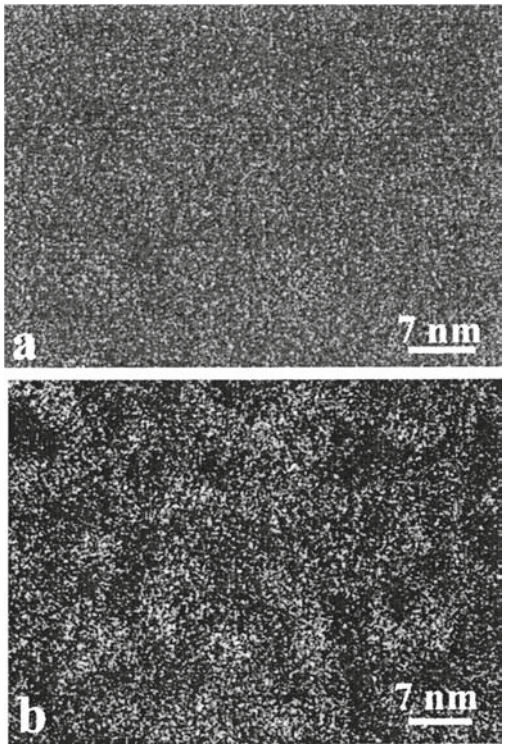

Figure 14. EELS carbon mappings from (a) TEOS-only and (b) Ac_2O samples.

Acknowledgments

Gratitude is expressed to the Swedish International Development Aid/Swedish Agency for Research Cooperation (SIDA/SAREC) for funding this project, and to the International Science Programmes (ISP) of Uppsala University for disbursement of funds and hospitality. The Solid State Division, Materials Engineering Department is thanked for providing laboratory space. The University of Zimbabwe is also thanked for granting duty leave to one of us.

References

1. Xiaohu Deng, Yinghong Yue, and Zi Gao, J. Colloid Interface Sci. **206**, 52 (1998).
2. Y.X. Wang, S.H. Tan, D.L. Jiang, and X.Y. Zhang, Carbon **41**, 2065 (2003).
3. Zhi-Guo Shi, Yu-Qi Feng, Li Xu, and Shi-Lu Da, Carbon **41**, 2668 (2003).
4. J. Li, L.S. Chia, N.K. Goh, and S.N. Tan, J. Electroanal. Chem. **460**, 234 (1999).
5. A.J.G. Zarbin, R. Bertholdo, and M.A.F.C. Oliveira, Cabon **40**, 2413 (2002).
6. S. Han, M. Kim, and T. Hyeon, Carbon **41**, 1525 (2003).
7. Y. Matsai, S. Polarz, and M. Antonietti, Adv. Funct. Mater. **12**, 197 (2002).
8. E. Wäckelgård, G.A. Niklasson, and C.G. Granqvist, in *Solar Energy: The State of the Art*, edited by Gordon Jeffrey (James and James (Science Publishers) Ltd., United Kingdom, 2001). p. 112.
9. G.A. Niklasson and C.G. Granqvist, in *Materials Science for Solar Energy Conversion Systems*, edited by C.G. Granqvist (Pergamon Press, Oxford 1991), p. 70s.
10. M. Farooq and Z.H. Lee, Renewable Energy **28**, 1421 (2003).
11. E. Wäckelgård and G. Hultmark, Solar Energy Mater. **54**, 165 (1998).
12. J. Vince, A.S. Vuk, U.O. Krasovec, B. Orel, M. Kohl, and M. Heck, Sol. Energy Mater. **79**, 313 (2003).
13. T. Boström, E. Wäckelgård, and G. Westin, Solar Energy **74**, 497 (2003).
14. N Etherden, T. Tesfamichael, G. Niklasson, and E. Wäckelgård, J. Phys. D: Appl. Phys. **37**, 1 (2004).
15. E.M. Rabinovich, in *Sol-Gel Optics: Processing and Applications*, edited by L.C. Klein (Kluwer Academic Publishers, Boston, 1994) chapter 1.
16. J. Livage, F. Babonneau, and C. Sanchez, in *Sol-Gel Optics: Processing and Applications*, edited by L.C. Klein (Kluwer Academic Publishers, Boston, 1994) Chapter 2.
17. W. Que, et. al., Thin Solid Films **359**, 177 (2000).
18. A.V. Rao, R.R. Kalesh, and G.M. Pajonk, J. Mater. Sci. **38**, 4407 (2003).
19. I.M. Thomas, in *Sol-Gel Optics: Processing and Applications*, edited by L.C. Klein (Kluwer Academic Publishers, Boston, 1994) Chapter 6.
20. C.J. Brinker and G.W. Scherer, *Sol-Gel Science: The Physics and Chemistry of Sol-Gel Processing* (Academic Press, San Diego, 1990) Chapter 8.